THE JOURNAL OF BIOLOGICAL CHEMISTRY
Vol. 272, No. 52, Issue of December 26, pp. 32817–32823, 1997

Printed in U.S.A.

Multimer Formation and Ligand Recognition by the Long Pentraxin PTX3

SIMILARITIES AND DIFFERENCES WITH THE SHORT PENTRAXINS C-REACTIVE PROTEIN AND SERUM AMYLOID P COMPONENT*

(Received for publication, August 6, 1997, and in revised form, October 6, 1997)

Barbara Bottazzi‡§, Valérie Vouret-Craviari‡§, Antonio Bastone‡§, Luca De Gioia‡, Cristian Matteucci‡, Giuseppe Peri‡, Fabio Spreafico‡, Mario Pausa¶, Cinzia D'Ettorre‖, Elisabetta Gianazza, Aldo Tagliabue‖, Mario Salmona‡, Francesco Tedesco‡‡, Martino Introna‡, and Alberto Mantovani‡§§¶¶**

‡*From the Istituto di Ricerche Farmacologiche "Mario Negri," Via Eritrea 62, 20157 Milano, Italy;* ¶*Istituto di Ostetricia e Ginecologia, IRCCS Burlo Garofolo, Trieste, Italy;* ‖*DOMPE' S.P.A., L'Aquila, Italy;* **Istituto di Scienze Farmacologiche, Università di Milano, Milan, Italy;* ‡‡*Dipartimento di Fisiologia e Patologia, Università di Trieste, Trieste, Italy; and* §§*Sezione di Patologia e Immunologia, Dipartimento di Biotecnologie, Università di Brescia, Brescia, Italy*

PTX3 is a prototypic long pentraxin consisting of a C-terminal 203-amino acid pentraxin-like domain coupled with an N-terminal 178-amino acid unrelated portion. The present study was designed to characterize the structure and ligand binding properties of human PTX3, in comparison with the classical pentraxins C-reactive protein and serum amyloid P component. Sequencing of Chinese hamster ovary cell-expressed PTX3 revealed that the mature secreted protein starts at residue 18 (Glu). Lectin binding and treatment with *N*-glycosidase F showed that PTX3 is *N*-glycosylated, sugars accounting for 5 kDa of the monomer mass (45 kDa). Circular dichroism analysis indicated that the protein consists predominantly of β-sheets with a minor α-helical component. While in gel filtration the protein is eluted with a molecular mass of ≅900 kDa, gel electrophoresis using nondenaturing, nonreducing conditions revealed that PTX3 forms multimers predominantly of 440 kDa apparent molecular mass, corresponding to decamers, and that disulfide bonds are required for multimer formation. The ligand binding properties of PTX3 were then examined. As predicted based on modeling, inductive coupled plasma/atomic emission spectroscopy showed that PTX3 does not have coordinated Ca^{2+}. Unlike the classical pentraxins CRP and SAP, PTX3 did not bind phosphoethanolamine, phosphocholine, or high pyruvate agarose. PTX3 in solution, bound to immobilized C1q, but not C1s, and, reciprocally, C1q bound to immobilized PTX3. Binding of PTX3 to C1q is specific and saturable with a K_d 7.4×10^{-8} M as determined by solid phase binding assay. The Chinese hamster ovary cell-expressed pentraxin domain bound C1q when multimerized. Thus, as predicted on the basis of computer modeling, the prototypic long pentraxin PTX3 forms multimers, which differ from those formed by classical pentraxins in terms of protomer composition and requirement for disulfide bonds, and does not recognize CRP/SAP ligands. The capacity to bind C1q, mediated by the pentraxin domain, is consistent with the view that PTX3, produced in tissues by endothelial cells or macrophages in response to interleukin-1 and tumor necrosis factor, may act as a local regulator of innate immunity.

Pentraxins (C-reactive protein, CRP,[1] and serum amyloid P component, SAP) are acute phase proteins conserved during evolution from *Limulus polyphemus* to man (1–6). Pentraxins are composed of monomers with a β-jelly roll topology that usually assemble into pentameric, noncovalently associated structures (7–9). CRP and SAP are made in the liver in response to inflammatory mediators, most prominently interleukin-6 (10, 11). A number of ligands, recognized in a calcium-dependent manner, have been identified for CRP and SAP, including phosphoethanolamine (PE), phosphocholine (PC) (12), DNA and chromatin (13–15), immune complexes, various sugars (16), the best characterized of which is methyl 4,6-*O*-(1-carboxyethylidene)-β-D-galactopyranoside (MOβDG) (17), and complement components (13, 18–22). Moreover, SAP binds to all forms of amyloid fibrils (23) and, in addition, to fibronectin, C4-binding protein (24, 25), and glycosaminoglycans (26). Pentraxins represent a mechanism of innate resistance against microbes, tools to scavenge cellular debris and components of the extracellular matrix as illustrated by amyloid deposits (3).

PTX3 is a prototypic long pentraxin, structurally related to, yet distinct from, classical pentraxins. PTX3 was cloned as an interleukin-1-inducible gene in endothelial cells (27) and as a tumor necrosis factor-inducible gene (TSG 14) in fibroblasts (28). PTX3 is constituted of a C-terminal pentraxin-like domain of 203 amino acids encoded by the third exon and by an N-terminal 178- amino acid long portion (27). Inflammatory cytokines induce PTX3 expression in a variety of cell types, most prominently endothelial cells and mononuclear phagocytes (27, 29–31). After cloning of PTX3, other "long pentraxins" were identified, including guinea pig apexin (32, 33), XL-PXN1 from

* This work was supported by the Associazione Italiana Ricerca sul Cancro (AIRC), by the special project Biotechnology, Consiglio Nazionale delle Ricerche (CNR), by Istituto Superiore di Sanità (project Oncology), and by Ministero della Ricerca Scientifica e Tecnologica (40 and 60%), Italy. The costs of publication of this article were defrayed in part by the payment of page charges. This article must therefore be hereby marked "*advertisement*" in accordance with 18 U.S.C. Section 1734 solely to indicate this fact.

§ These authors have contributed equally to this work.

¶¶ To whom correspondence should be addressed: Fax: 39/2/3546277; E-mail: Mantovani@IRFMN.MNEGRI.IT.

[1] The abbreviations used are: CRP, C-reactive protein; SAP, serum amyloid P component; PE, phosphoethanolamine; PC, phosphocholine; MOβDG, methyl 4,6-*O*-(1-carboxyethylidene)-β-D-galactopyranoside; PBS, phosphate-buffered saline; HPA, high pyruvate agarose; NP, neuronal pentraxin; bp, base pair(s); CHO, Chinese hamster ovary; PAGE, polyacrylamide gel electrophoresis; DTT, dithiotreitol; RU, resonance units.

Xenopus (34), rat neuronal pentraxin (NP) (35), human neuronal pentraxin (NPTX2) (36), which possibly represents the human homologue of apexin, and Narp (37), which possibly represents the rat homologue of apexin. In all these molecules a C-terminal pentraxin domain is coupled to diverse, unrelated N-terminal portions (32–36). The structure and function of long pentraxins is unknown.

The present study was designed to express the prototypic long pentraxin PTX3 in an eukaryotic system and to characterize its structure and ligand recognition in comparison to classical pentraxins. In particular, experiments were designed to test predictions made on the basis of modeling of the pentraxin domain of PTX3 on the three-dimensional structure of SAP (31).

EXPERIMENTAL PROCEDURES

Production of Recombinant PTX3—A 1311-bp fragment of human PTX3 cDNA, containing the complete coding sequence, was subcloned in pSG5 vector (Stratagene, La Jolla, CA) and transfected in CHO cells by calcium phosphate precipitation. Two clones selected with G418 (Life Technologies, Inc., Paisley, Scotland, UK) were used in the present study, CHO 3.5, producing high levels of PTX3, and CHO 2.1, transfected with the antisense construct. Conditioned medium was collected from confluent monolayers incubated 24 h with culture medium (Dulbecco's modified Eagle's medium; Seromed, Berlin, Germany) without fetal calf serum. The pentraxin domain of PTX3 was obtained by introduction by polymerase chain reaction of a *Xho*I site at the end of the signal peptide (position 18 of the published sequence) (27) and at the 5′ end of the pentraxin domain (position 172). The fragment was subcloned in pSG5 vector and transfected in CHO cells by calcium phosphate precipitation as described above. A high recombinant producer clone, named sPTX3, was selected.

Gel Electrophoresis and Western Blot Analysis—5–10% polyacrylamide gradient gel in the presence of SDS was run in the discontinuous buffer system of Laemmli (38). Gels were stained with Amido Black, Coomassie Brilliant Blue, or silver nitrate (39). For Western blots, separated proteins were electroblotted onto nitrocellulose filters (Hybond ECL, Amersham Corp.) and labeled with anti-PTX3 monoclonal antibody (see below) following standard procedures. Labeled proteins were detected by enhanced chemiluminescence (ECL, Amersham Corp.) in accordance with the manufacturer's instructions. PTX3 was analyzed in the native state in 5–10% gradient polyacrylamide gel electrophoresis (PAGE).

Protein Purification—Culture supernatant from CHO 3.5 cells was concentrated, and the buffer was changed to 50 mM imidazole, pH 6.6, before application on a HR 5/5 Mono Q column (Pharmacia Biotech, Uppsala, Sweden) preequilibrated with the same buffer. The column was washed until the absorbance was stable, and PTX3 was eluted with 1 M NaCl in 50 mM imidazole at 1 ml/min using a nonlinear gradient. In the first step, the NaCl concentration was increased from 0% to 58% in 35 min. Then the NaCl concentration was immediately increased to 100%, and PTX3 was obtained as a narrow peak as monitored by UV detection at 280 nm. The PTX3-containing fraction was subjected to gel filtration on Sephacryl S-300, and PTX3 was finally eluted with PBS. The purification of PTX3 was monitored by SDS-PAGE and Western blot analysis. To further control the elution profile, purified PTX3 was applied to a Superose 6 column (Pharmacia Biotech) calibrated with molecular weight standards and eluted with PBS at a flow rate of 0.4 ml/min. Elution was monitored by UV detection at 280 nm, and fractions (2 min each) were subsequently analyzed on native PAGE.

Antibodies—A rat (16B5) and mouse (1C8) antibody against human PTX3 were used in this study. Rabbit antiserum to human C1q was purchased from Istituto Behring SpA (Scoppito, Italy), and biotin-labeled goat anti-rabbit IgG was obtained from Sigma.

Lectin Staining and Deglycosylation—Purified PTX3 (5 μg) after SDS-PAGE and electroblotting was incubated with the following lectin-peroxidase conjugates at a concentration of 50 μg/ml: concanavalin A, wheat germ agglutinin, *Bandeiraea simplicifolia* lectin BS-II, *Vicia faba* lectin, *Psophocarpus tetragonolobus* lectin, and *Tetragonolobus purpureas* lectin. The zymogram for peroxidase was developed according to Taketa (40) in a solution containing 2 mg/ml NADH, 0.6 mg/ml nitro blue tetrazolium, 0.4 mg/ml phenol, and 3 μl/ml H_2O_2, in phosphate buffer, pH 7.0. Purified PTX3 (160 μg in PBS) was first made 1% in SDS and incubated at 100 °C for 5 min, then diluted 5-fold with concentrated buffer to a final concentration of 50 mM sodium phosphate, pH 7.4, 1% Triton X-100, 0.1% SDS, and 1 unit of *N*-glycosidase F (Boehringer Mannheim GmbH, Mannheim, Germany). After overnight incubation at room temperature, samples were analyzed by SDS-PAGE.

Purification and Cross-linking of sPTX3—Supernatant from sPTX3 cells was concentrated by ultrafiltration, and the buffer was changed to 50 mM Tris-HCl, pH 7, before application on a HR 5/5 Mono Q column. sPTX3 was eluted with a linear gradient of NaCl (from 0 to 1 M) in 50 mM Tris-HCl. Fractions recognized by the 16B5 monoclonal antibody were pooled, concentrated by ultrafiltration, and subjected to cross-linking. sPTX3 (200 μg in 200 μl of Veronal-buffered saline) was cross-linked by adding 20 μl of 10 mM bis(sulfosuccinimidyl)suberate (Pierce) for 1 h at room temperature. Then 40 μl of Tris-buffered saline was added to stop the reaction.

Ligand Binding Assays—Binding of PTX3 with Sepharose-immobilized PE, Sepharose-immobilized PC, or high piruvate agarose (HPA) was performed as described previously for CRP and SAP (41). The presence of PTX3 was assayed by Western blot, and results are expressed as area under the curve after densitometric analysis of the exposed film performed by the scanning densitometer GS300 (Hoefer Scientific Instrument, San Francisco, CA). As a control, acute phase human serum was incubated in parallel with immobilized ligand and processed as for PTX3, then assayed for the presence of CRP and/or SAP by electroimmunoassay as described previously (41).

Binding of PTX3 to C1q was performed as described previously for CRP and SAP (19, 20). Briefly 96-well plates were coated with 250–500 ng of C1q (Calbiochem) in PBS with calcium and magnesium (4 °C overnight). Wells were washed with PBS plus 0.05% Tween 20, blocked with 0.5% dry milk in PBS (2 h at room temperature), and extensively washed before the addition of 100 μl of supernatant from 3.5 or 2.1 cell lines or 200 ng of purified PTX3 diluted in PBS (30 min, 37 °C). After washing, plates were incubated with 16B5 monoclonal antibody (1 h at room temperature), washed again, and incubated with horseradish peroxidase-labeled goat anti-rat IgG (Amersham; 1:2000; 1 h at room temperature). After extensive washing, 100 μl of chromogen substrate ABTS were added (Kirkegaard and Perry, Gaithersburg, MD), and absorbance values were read at 405 nm. As positive control for the binding assay, immobilized rabbit IgG heated at 63 °C for 20 min immediately prior to use was used (Agg-IgG) (42).

In another set of experiments, wells were coated by overnight incubation at 4 °C with 200 μl of purified PTX3 (2.5–10 μg/ml) in 100 mM sodium carbonate, pH 9.6. After blocking, C1q was added in amounts varying between 0.125 and 2 μg/ml, and incubation was continued for 1 h at 37 °C. The bound C1q was revealed by its reaction with a specific rabbit antibody for 1 h at 37 °C followed, after washing, by biotin-labeled goat anti-rabbit IgG for an additional h at 37 °C. The wells were washed and incubated with 200 μl of alkaline phosphatase-conjugated streptavidin (Jackson Laboratories, West Grove, PA) diluted 1/8000 for 30 min at 37 °C. The enzymatic reaction was developed using the substrate *p*-nitrophenyl phosphate (Sigma; 1 mg/ml) in 0.1 M glycin buffer pH 10.4 containing 0.1 mM $MgCl_2$ and 0.1 mM $ZnCl_2$. In some experiments C1q purified from human plasma following the procedure originally described by Tenner *et al.* (43) was used with similar results.

Binding of PTX3 to C1q was characterized using biotin-labeled purified PTX3 (bPTX3). Concentrations ranging from 25 to 800 ng of bPTX3 (0.56–17.92 pmol considering a molecular mass of 45 kDa for PTX3 monomer) in 100 μl were added to triplicate wells coated with 200 ng of C1q (0.49 pmol). After 1 h incubation at 37 °C, bound PTX3 was detected with horseradish peroxidase-labeled avidin (1/2000, 1 h) and chromogen substrate ABTS, as described. The results were converted to picomolar concentration using a standard curve of bPTX3 and considering a molecular mass of 45 kDa for PTX3 monomer. K_d and B_{max} were obtained by nonlinear fitting of the saturation curves (44). Binding of bPTX3 to type IV collagen (Sigma; 10 μg/ml), fibronectin (Sigma; 10 μg/ml), and gelatin (Sigma; 0.5%) was analyzed with essentially the same protocol.

Biosensor Analysis—The interaction of PTX3 with C1q was also analyzed with the BIAcore® system (biomolecular interaction analysis; BIAcore AB, Uppsala, Sweden). C1q was immobilized on a CM5 sensor chip (Pharmacia Biosensor) using the amine coupling kit (Pharmacia Biosensor) (45). A volume of 30 μl of ligand (10 μg/ml C1q in 10 mM sodium acetate, pH 4.1) was immobilized with a continuous flow of HBS (10 mM HEPES, 150 mM NaCl, 3.4 mM EDTA, and 0.05% BIAcore® surfactant P20, pH 7.4) at 5 μl/min. Each binding assay was performed with a constant flow rate (5 μl/min) of HBS, pH 7.4 at 25 °C. The analyte PTX3 was injected over the ligand surface in HBS and the surface was then regenerated by injection of 5 μl of 25 mM NaOH. Analyte binding was calculated as the difference in RU before and after the interaction of ligand with analyte. For saturation analysis, PTX3

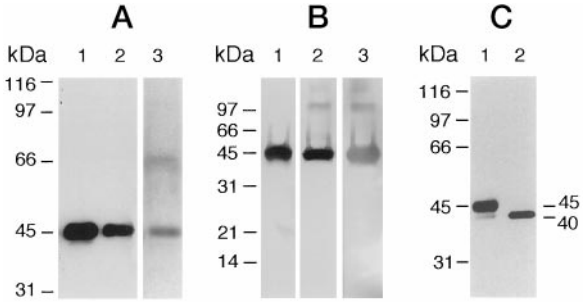

FIG. 1. **Purification and glycosylation of PTX3 expressed in CHO cells.** *Panel A*, proteins were separated on 4–10% SDS-PAGE and analyzed by Western blotting (*lanes 1* and *2*) and silver staining (*lane 3*). *Lane 1*, supernatant from CHO 3.5 cells; *lanes 2* and *3*, the same after purification. *Panel B*, purified protein was run on 7.5–17.5% SDS-PAGE and stained with Amido Black (*lane 1*), concanavalin A (*lane 2*), or wheat germ agglutinin (*lane 3*). *Panel C*, effect of enzymatic deglycosylation on PTX3. Purified PTX3 was denatured by SDS and incubated in the absence (*lane 1*) or presence of *N*-glycosidase F (*lane 2*) overnight at room temperature. Control and enzyme-treated samples were analyzed by Western blot after SDS-PAGE. The molecular mass standards ($\times 10^{-3}$) are indicated on the *left*.

was serially diluted in HBS to concentrations ranging from 20 to 600 nM. Each sample (30 μl) was injected and allowed a total contact time with the ligand surface of 6 min.

RESULTS

Production and Purification of Human Recombinant PTX3—The culture supernatant of the CHO 3.5 cell line was analyzed by SDS-PAGE under reducing conditions, and a protein with an apparent molecular mass of 45 kDa, which was not present in the culture supernatant from the antisense clone 2.1 (not shown), was observed. Western blot analysis of the same culture supernatant showed that this protein is recognized by the monoclonal anti-PTX3 antibody 16B5 (Fig. 1, *panel A*, *lane 1*).

To purify the protein, 500 ml of culture supernatant from CHO 3.5 cells were collected, concentrated by ultrafiltration, and then subjected to ion exchange chromatography on a Mono Q column. The fractions containing PTX3 were subsequently subjected to gel filtration in PBS. The process of purification was monitored by SDS-PAGE and by microsequence analysis (see below). The purification scheme yielded PTX3 preparations of considerable purity (Fig. 1, *panel A*, *lanes 2* and *3*) with an occasional 66-kDa contaminant. About 5 mg of pure PTX3 were routinely obtained from 500 ml of conditioned medium. Microsequence analysis, performed on two occasions on the N terminus of the purified protein, confirmed the purity and showed identity with the amino acid sequence predicted on the basis of the cDNA (Glu-Asn-Ser-Asp-Asp-Tyr-Asp-Leu-Met-Tyr-Val-Asn-Leu-Asp-Asn-Glu-Ile); it demonstrates that the predicted leader peptide is removed when the protein is secreted, the first sequenced amino acid being Glu^{18} of the published sequence (27, 31).

Glycosylation—The amino acid sequence predicts a molecular mass for the reduced protein of 40 kDa instead of the 45 kDa observed in SDS-PAGE. The PTX3 sequence shows the presence of a potential *N*-linked glycosylation site at amino acid position 220 (27). SDS-PAGE of the reduced protein shows the presence of two closely related bands (Fig. 1, *panels A* and *C*). The lower band has a calculated molecular mass of 40 kDa, the size expected for PTX3 on the basis of the amino acidic sequence without the leader peptide. The amount of 40-kDa material was variable from preparation to preparation. It is noteworthy that the same two bands were present in supernatants of stimulated endothelial cells and monocytes, with considerable donor to donor variation (29).[2] To test for the presence of oligosaccharides, PTX3 was stained with different lectin-peroxidase conjugates. PTX3 showed a strong staining for peroxidase-conjugated concanavalin A (specific for α-D-mannose and α-D-glucose) and wheat germ agglutinin (specific for (D-GlcNAc)2NeuAc, Fig. 1, *panel B*) while it was not stained by *B. simplicifolia*, *V. faba*, *P. tetragonolobus*, and *T. purpureas* (data not shown).

To better characterize the glycosylation of PTX3, the purified protein was treated with *N*-glycosidase F, an enzyme that cleaves Asn-linked high mannose as well as hybrid and complex oligosaccarides, and the deglycosylation was monitored as an increase in electrophoretic mobility. As shown in Fig. 1, *panel C*, after treatment with *N*-glycosidase F, PTX3 exhibited a decrease of approximately 5 kDa, from 45 to 40 kDa. It is concluded that PTX3 is glycosylated and that *N*-linked sugars account for 5 kDa of the major 45-kDa PTX3 protomer. Isoelectrofocusing of purified PTX3 showed five different bands with a pI ranging from 4.5 to 4.65 (data not shown), possibly indicating heterogeneity in glycosylation in agreement with a previous suggestion (29).

Conformation and Multimer Formation—The purified material was used to generate a CD spectrum to determine the possible conformation of the protein. The spectrum is characterized by a positive band at 199 nm and a negative band at 217 nm. Careful observation of the negative band shows the presence of shoulders at 209 and 224 nm. Spectral deconvolution indicates a predominantly β-sheet protein, with some contribution of α-helical structure (data not shown).

Classical pentraxins form noncovalently linked multimers (7–9). In an effort to obtain indications as to the capacity of PTX3 to form multimers, purified protein was analyzed by gel filtration on Superose 6. As shown in Fig. 2, *panel A*, on gel filtration PTX3 eluted with an apparent molecular mass of about 900 kDa (similar results were obtained also with Sephacryl S300). When fractions from gel filtration containing the protein were run on a native gel, a pattern similar to that shown in Fig. 2, *panels D* and *E* (see below) was observed.

To further characterize the PTX3 multimers, denaturation with SDS and reduction with DTT were used. The apparent size of the PTX3 multimers was determined by gel electrophoresis followed by staining or Western blotting. In the absence of reducing agents, SDS treatment caused disassembly of the multimers formed by SAP (not shown) and CRP (Fig. 2, *panel B*), to their constituent monomers. In contrast, under the same conditions, SDS treatment in the absence of DTT did not disaggregate PTX3, which migrated as two high molecular mass bands that barely entered the gel (Fig. 2, *panels B* and *C*). SAP multimers are clearly visible under nondenaturing, nonreducing conditions as a major 230-kDa band (Fig. 2, *panel D*). Under the same native conditions PTX3 migrates in the gel as a predominant 440-kDa apparent molecular mass species, possibly corresponding to a decamer, as revealed by direct staining and Western blotting (Fig. 2, *panels D* and *E*). In addition, two minor higher forms in the 540–600 kDa range were usually visible. This relative distribution of different multimeric forms was observed both in silver-stained gel and in Western blot (Fig. 2, *panel D* and *E*) and is not dependent on concentration, since gel filtration and PAGE performed with diluted PTX3 (up to the sensitivity of these assays) gave similar results (not shown). When PTX3 was incubated with increasing concentrations of DTT prior to SDS-PAGE, progressively smaller aggregates were observed until, at 1 mM DTT, all protein ran in the form of the 45-kDa protomer (not shown).

[2] N. Polentarutti and M. Introna, unpublished results.

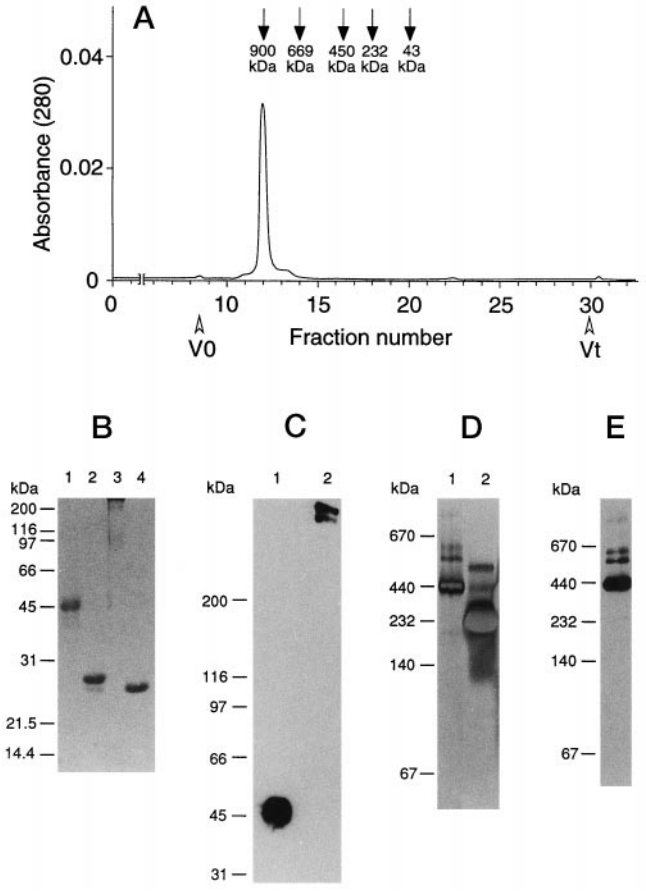

FIG. 2. **Multimer formation by PTX3.** *Panel A* shows the elution profile of PTX3 submitted to gel filtration on Superose 6 and eluted as detailed under "Experimental Procedures." *Arrows* indicate molecular mass markers (ovalbumin, 43 kDa; catalase, 232 kDa; ferritin, 450 kDa; thyroglobulin, 669 kDa; rabbit IgM, 900 kDa). Purified PTX3 was analyzed on denaturing (*panels B* and *C*) or native (*panels D* and *E*) gel. *Panel B* (Coomassie Blue-stained gel): *lane 1*, reduced PTX3; *lane 2*, reduced CRP; *lane 3*, unreduced PTX3; *lane 4*, unreduced CRP. *Panel C* (Western blot): *lane 1*, reduced PTX3; *lane 2*, unreduced PTX3. *Panel D* (silver-stained gel): *lane 1*, unreduced PTX3; *lane 2*, unreduced SAP. *Panel E*: Western blot of unreduced native PTX3.

Calcium—To investigate the possible presence of Ca^{2+} strongly coordinated to specific sites of the protein (as in SAP and CRP) inductive coupled plasma/atomic emission spectroscopy experiments were performed using protein samples purified in Ca^{2+}-free buffers. The emission profiles clearly show that the Ca^{2+} content of the protein is comparable to that of a control, indicating that PTX3 does not have a specific coordination site for Ca^{2+} (data not shown).

Ligands—We analyzed the binding of PTX3 to the classical ligands recognized by CRP and SAP, namely PE, PC, and HPA (MOβDG). As shown in Fig. 3, PTX3 does not appreciably bind any of these ligands, that, on the contrary, are recognized by CRP and/or SAP.

A well known ligand for both CRP and SAP is the collagen-like C1q molecule, a component of the complement system. The interaction of soluble PTX3 with immobilized C1q was analyzed, and a dose-dependent binding of PTX3 was observed, which, on the contrary, did not react with bound C1s used as a control for nonspecific binding (Fig. 4, *panel A*). The data were essentially similar when either the spent medium of CHO cells transfected with the sense cDNA for PTX3 or the purified protein were assayed. Under these conditions PTX3 did not bind type IV collagen, fibronectin, and gelatin (Fig. 4, *panel B*), while binding to H1 histone was observed (data not shown). Binding of PTX3 to C1q was also observed when soluble C1q was tested on immobilized PTX3 (Fig. 4, *panel C*).

To characterize the binding of PTX3 to C1q, serial dilutions of biotinylated PTX3 were added to immobilized C1q and the amount of bound PTX3 evaluated on the basis of a standard curve of the biotinylated protein. Fig. 4, *panel D*, represents a typical experiment showing the binding of PTX3 to C1q; the binding is saturable with a K_d of 7.4×10^{-8} M and B_{max} 1.1 pmol PTX3/pmol C1q (assuming for PTX3 the mass of the monomer, 45 kDa; mean of three independent experiments). Similar results were obtained also when nonbiotinylated purified PTX3 was used. Results obtained using biotinylated PTX3 were confirmed in preliminary experiments where binding of unlabeled PTX3 to C1q was investigated by means of real time biomolecular interaction analysis with BIAcore®. As shown in Fig. 5, *panel A*, when C1q was immobilized on the sensor chip it was possible to observe a significant binding of PTX3, which was subsequently recognized by the specific antibody 1C8. Kinetic analysis of the interaction between the two molecules (Fig. 5, *panel B*) allowed to calculate a K_{on} of 2.4×10^5 M^{-1} s^{-1} and a K_{off} of 4×10^{-4} s^{-1}.

The Role of the Pentraxin Domain—We wanted to obtain preliminary indications as to the role of the pentraxin domain of PTX3 in multimer formation and ligand recognition. A mutant consisting of the PTX3 pentraxin domain (starting from aa 179 of the mature protein, called short PTX3, sPTX3) was expressed in CHO cells. As shown in Fig. 6, *panel A*, sPTX3 migrated in SDS-PAGE under reducing conditions as two bands of 23 and 28 kDa. The 28-kDa band was drastically reduced by treatment with *N*-glycosidase F as described above for PTX3 (data not shown). Therefore, the two bands most likely represent unglycosylated and glycosylated sPTX3, consistent with the observation that the *N*-linked glycosylation site is located within the pentraxin domain at aa 220 of the mature protein. Native sPTX3 did not form large multimers (decamers) and did not bind to C1q (Fig. 6, *panel B*). It is well known that the classical short pentraxins CRP and SAP required cross-linking for binding to C1q (13). As expected on this basis, cross-linked sPTX3, consisting of multimers from ≅60- to ≅220-kDa apparent molecular mass (data not shown), did bind C1q but not C1s. It is concluded that the recognition of C1q by PTX3 requires multimer formation and is mediated by the pentraxin domain of the molecule.

DISCUSSION

The present investigation was designed to express in mammalian cells and to characterize the prototypic long pentraxin PTX3 and to compare its properties to those of classical pentraxins. The first amino acid of human PTX3 expressed and secreted by CHO cells is Glu^{18} of the cDNA-deduced sequence, after removal of a signal peptide as predicted (27). The secreted protein consists of a major 45-kDa form of the protomer, with a minor 40-kDa component. Lectin binding and *N*-glycosidase treatment suggest that the 45-kDa form is glycosylated and that sugar moieties, presumably bound to the *N*-glycosylation site Asn^{203} (from now on residue numbering is based on mature protein, without the leader peptide), account for 5 kDa.

A major objective of the present study was to test structural and functional predictions made in a previous investigation in which PTX3 was modeled on the three-dimensional structure of SAP (7, 31). The pentraxin domain of PTX3 is accommodated comfortably in the three-dimensional scaffold of SAP, a consequence of the considerable degree of amino acid overall conservation between the molecules (≅50%). Nonetheless, several differences were highlighted, which could now be tested experimentally. In addition to the two Cys residues at position 193 and 254 (respectively 36 and 95 of SAP numbering) (31) con-

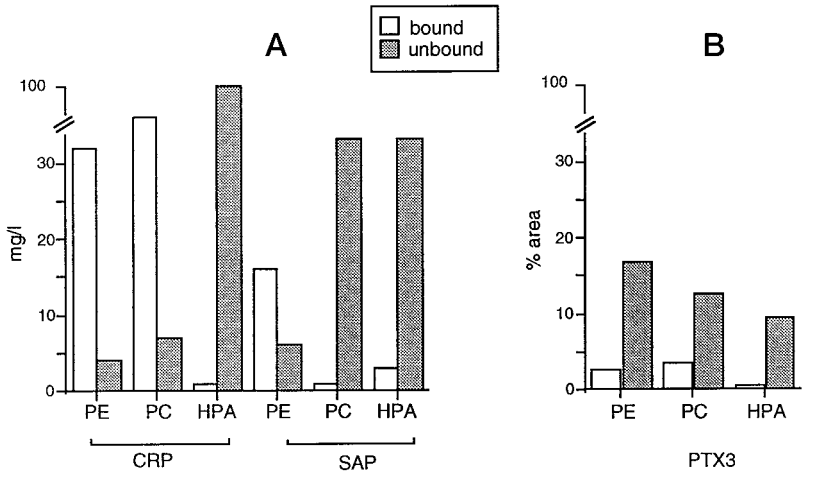

FIG. 3. **Binding of PTX3 to PE, PC, or HPA.** *Panel A* shows the binding of CRP and SAP to the classical pentraxin ligands immobilized to Sepharose. Data are expressed as milligrams/liter of the different proteins present in the bound or unbound fractions as evaluated by immunoassay. *Panel B* shows the binding of PTX3 to the same ligands; data are expressed as area under the curve after densitometric analysis of the exposed film, as detailed under "Experimental Procedures."

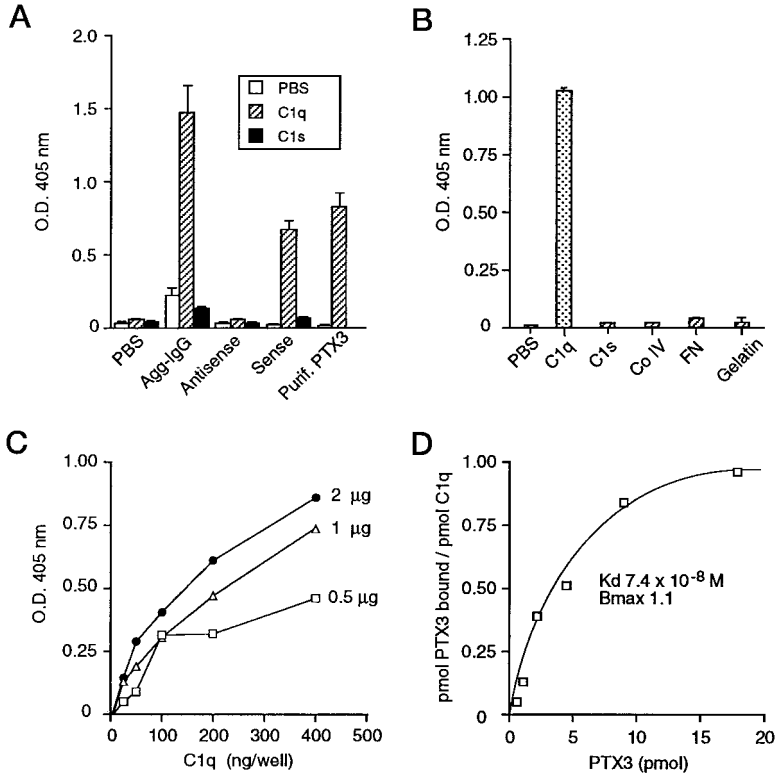

FIG. 4. **Binding of PTX3 to immobilized C1q, type IV collagen, fibronectin, and gelatin.** *Panel A* shows the binding of supernatant from transfected and control cells and of purified PTX3. C1q was immobilized on polystyrene plates and incubated with PTX3 or Agg-IgG for 30 min at 37 °C. Binding was revealed by specific antibodies and enzyme-linked immunosorbent assay. *Panel B*, 100 µl of type IV collagen (*Co IV*, 10 µg/ml), fibronectin (*FN*) (10 µg/ml), or gelatin (0.5%) were immobilized on plastic wells. Binding with biotinylated PTX3 (250 ng, 2 h at 37 °C) was analyzed as detailed under "Experimental Procedures." *Panel C* demonstrates the binding of C1q to immobilized PTX3. Different concentrations of purified PTX3 were immobilized on plastic plates and incubated with different amount of C1q for 1 h at 37 °C. S.E. for data of *panel C* was less than 0.05%. *Panel D* shows the specific binding of PTX3 to C1q. C1q was immobilized on plastic wells and incubated with different amounts of biotinylated PTX3. Specific binding was measured in accordance with a standard curve of biotinylated PTX3.

served in all known members of the pentraxin family cloned so far, PTX3 (human and mouse) shows four additional Cys in the pentraxin domain and three in the non-pentraxin N-terminal portion. Cys^{162} and Cys^{340} were suggested to form an additional intramolecular bridge, whereas the two tandems (positions 30 and 32, 300 and 301) as well as Cys^{86} could engage in inter- or intramolecular bonds (31). Multimers of human CRP and SAP are noncovalently linked and, as expected, denaturing conditions cause disaggregation and monomer formation (Fig. 2, *panel B*) (7–9). Residues involved in multimer formation in CRP and SAP are not conserved in PTX3 (31). Accordingly, denaturing with SDS did not disassemble the PTX3 440-kDa multimers, and reduction with DTT was required for disaggregation to the 45-kDa protomer. Similar results have been described for apexin, another member of the long pentraxin group (32, 33). Other classical pentraxins may have disulfide bridges among the monomers, including plaice (46), dogfish (47, 48), *Xenopus* (49), *Limulus* (50, 51), and rat CRP (52, 53). The latter is unique among the proteins of this family, since there is an interchain disulfide bridge between some, but not all, subunits.

Classical pentraxins are multimeric proteins composed of variable numbers of subunits (1, 3). For instance human CRP is a pentamer, as is generally the case for members of the family, although SAP is composed of two pentameric disks interacting face-to-face and *Limulus* CRP is a hexamer (50, 54, 55). We found no evidence for pentamer formation by PTX3. Gel electrophoresis under nonreducing nondenaturing conditions showed a major aggregate with an apparent molecular mass of approximately 440 kDa, suggesting that in this condition the major PTX3 species is a decamer. Interestingly, comparison of PTX3 with SAP revealed changes in all amino acids involved in interprotomer interactions (31). Based on this structural consideration, it was therefore not surprising to find that PTX3 multimers differed considerably from the pentamer structure. On gel filtration, PTX3 eluted with an apparent molecular mass of approximately 900 kDa, whereas on native gel electrophoresis the apparent size of the multimer was 440 kDa. Such a discrepancy is not without precedent for pentraxins and

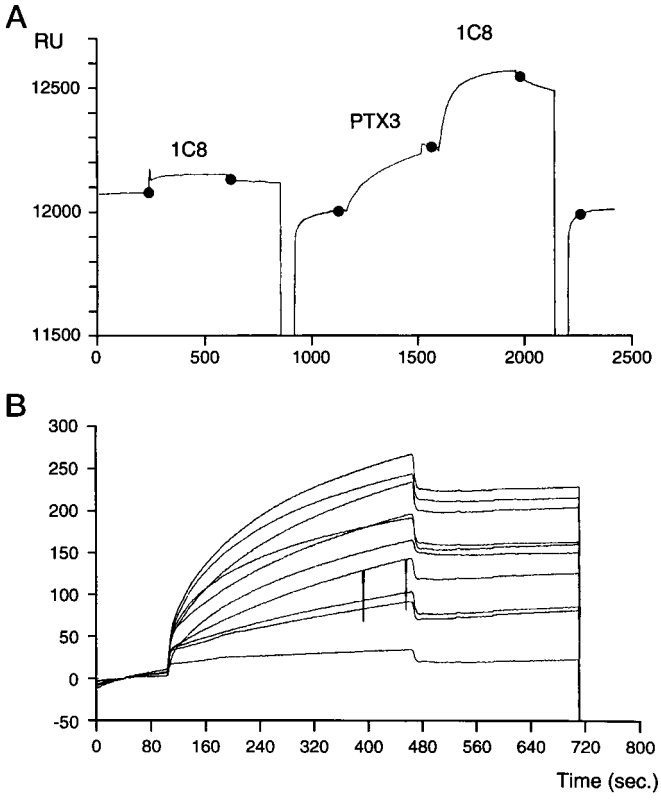

FIG. 5. **Specific interaction between C1q and PTX3 assessed with BIAcore®.** *Panel A*, sensorgrams from a representative experiment are reported. Each pair of *dots* indicates the beginning and the end of analyte injection, by which the increase in RU is calculated. Sensorgrams represent the interaction of immobilized C1q (base value 12,080 RU) with the anti-PTX3 antibody 1C8 (nonspecific binding of 54 RU; identical to that obtained on the sensor chip without C1q, data not shown) and with PTX3 (259 RU of binding). PTX3 bound to C1q was subsequently recognized by the specific antibody 1C8 (285 RU of binding). Regeneration of the surface with NaOH was performed twice, after 1C8 injection. *PanelB*, saturation analysis of PTX3 binding to C1q. Increasing concentrations of PTX3 (from 3 to 500 nM) were allowed to interact with immobilized C1q for 6 min, and association curves were recorded. Buffer was then run over and dissociation allowed to proceed. The kinetic parameters of the interaction were calculated for each sensogram. The mean values are K_{on} of 2.4×10^5 M^{-1} s^{-1}; K_{off} of 4×10^{-4} s^{-1}. Data are from a single experiment, representative of five performed.

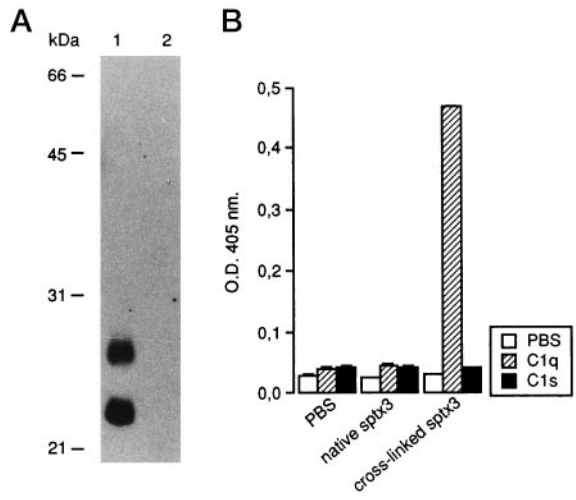

FIG. 6. **Binding of the pentraxin domain of PTX3 to C1q.** The pentraxin domain of PTX3, sPTX3, was analyzed on a reducing SDS-PAGE (*A*) and its binding to C1q was assessed (*B*). *Panel A*, Western blotting analysis: *lane 1*, 10-fold concentrated supernatant from sPTX3 transfected CHO cells; *lane 2*, 10-fold concentrated supernatant from antisense transfected CHO cells. Molecular mass markers are indicated on the *left*. *Panel B*, binding to C1q. PBS, C1q (500 ng/well), or C1s (500 ng/well) were immobilized on polystyrene plates and incubated with PBS, native sPTX3 (2 mg/well), or cross-linked sPTX3 (2 mg/well) for 30 min at 37 °C. Bound C1q was revealed as detailed under "Experimental Procedures."

molecules such as collectins (56). It is tempting to speculate that PTX3 is predominantly assembled as a decamer, with aggregates of two decamers being held by weak forces resolved upon electrophoresis.

SAP binds two Ca^{2+} ions per monomer (7). The amino acid residues of SAP involved in the binding of Ca^{2+} are not conserved in PTX3 (31). Inductive coupled plasma spectroscopy experiments show that purified PTX3 does not bind calcium as expected on the basis of structural analysis. Moreover, PTX3 does not seem to bind to PC, PE, and HPA, all classical calcium-dependent ligands of pentraxins (12, 17).

Circular dichroism spectroscopy, performed on purified PTX3, showed that the protein is characterized by a predominance of β-sheet secondary structure. Classical pentraxins are characterized by a very high amount of β-sheet secondary structure. Secondary structure prediction, performed on the N-terminal portion of PTX3 suggested a highly α-helical arrangement for this domain (31). Even if the presence of some α-helical component can be inferred from the CD spectral features of PTX3, the data suggest that the prediction overestimated the α-helical content of the protein.

Despite the structural and functional differences observed, PTX3 shares with CRP/SAP the ability to bind C1q, the first component of the classical pathway of complement activation. The binding was specific in that other complement components (C1s) and other proteins, including collagen type IV which binds SAP (57), were not recognized by PTX3. Using biotinylated PTX3, the estimated K_d was 7.4×10^{-8} M and a value in the same range was obtained when BIAcore® was used. B_{max} values indicate that one PTX3 protomer binds one C1q molecule. Using a similar methodological approach, a similar conclusion was reached when the interaction of SAP with collagen type IV was studied (57).

As predicted, recognition of C1q is mediated by the pentraxin domain of PTX3. C1q binding by the pentraxin domain requires multimer formation, as classically observed for the short pentraxins CRP and SAP (13). It was predicted that Cys at position 86 (mature protein) of the non-pentraxin portion may engage in interprotomer interactions (31). Artificial cross-linking of the isolated pentraxin domain of PTX3 (sPTX3), an absolute requirement for C1q recognition, may fulfill the same structural function as interprotomer Cys bonds do in the native molecule. Preliminary experiments indicate that PTX3 added to pooled human serum causes the consumption of C4 and of the total complement hemolytic activity[3] as expected on the basis of C1q binding. If PTX3 recognizes microbial components, as suggested by preliminary data,[4] in analogy with classical pentraxins, involvement of the complement system could regulate antimicrobial resistance, directly or indirectly via production of leukocyte chemotactic and activating fragments.

PTX3 is the first cloned member of the long pentraxin family, which includes XL-PXN1 from *Xenopus* (34), rat NP (35) and the three homologue genes guinea pig apexin (32, 33), human NTPX2 (36), and the latest rat neuronal pentraxin, Narp (37). No significant structural homologies are evident among the different non-pentraxin domains, and dendogram analysis of the pentraxin domain suggests that human PTX3 and murine PTX3 may be as distantly related to long pentraxins as to

[3] F. Tedesco and M. Pausa, unpublished results.
[4] B. Bottazzi and A. Bastone, unpublished results.

classical pentraxins.[5] It is interesting to observe that the long pentraxins do not have the restricted liver inducibility typical of CRP and SAP (upon interleukin-6 stimulation) and show a more promiscuous pattern of expression *in vitro* and *in vivo*. PTX3 can be expressed by endothelial cells, hepatocytes, fibroblasts, and monocytes in response to lipopolysaccharide and inflammatory cytokine (27, 29) and is induced by lipopolysaccharide *in vivo* in heart and lung but not in liver (30, 31).

The results reported here show that the long pentraxin PTX3 exhibits structural and functional similarities as well as differences when compared with the classical pentraxins CRP and SAP. PTX3 forms multimers as CRP and SAP do, but these differ in size and structural features (requirement for Cys bonds). PTX3 does not recognize the pentraxin ligands (Ca^{2+}, PE, PC, HPA) with the exception of C1q. This finding is consistent with the view that this pentraxin, secreted by macrophages and endothelial cells following stimulation with interleukin-1, tumor necrosis factor, and bacterial components, may contribute to the amplification of the effector mechanisms of innate immunity. In this regard, PTX3 seems to fulfill in tissues the same function that liver-derived CRP and SAP exert in the circulation. It remains to be elucidated whether and to what extent the observations reported herein for PTX3 can be extended to other recently identified long pentraxins.

Acknowledgments—We are grateful to Drs. Paul Proost and Jo Van Damme for one of the two microsequence analyses of the purified protein and to Professor Mark B. Pepys for help with the binding assay to Sepharose-immobilized ligands for measurement of CRP and SAP and for invaluable discussion. We also thank Dr. M. Gobbi for his help in the analysis of affinity and stoichiometry of PTX3 binding to C1q.

REFERENCES

1. Osmand, A. P., Friedenson, B., Gewurz, H., Painter, R. H., Hofmann, T., and Shelton, E. (1977) *Proc. Natl. Acad. Sci. U. S. A.* **74,** 739–743
2. Baltz, M. L., de Beer, F. C., Feinstein, A., Munn, E. A., Milstein, C. P., Fletcher, T. C., March, J. F., Taylor, J., Bruton, C., Clamp, J. R., Davies, A. J., and Pepys, M. B. (1982) *Ann. N. Y. Acad. Sci.* **389,** 49–75
3. Pepys, M. B., and Baltz, M. L. (1983) *Adv. Immunol.* **34,** 141–212
4. Gewurz, H., Zhang, X. H., and Lint, T. F. (1995) *Curr. Opin. Immunol.* **7,** 54–64
5. Kolb Bachofen, V. (1991) *Immunobiology* **183,** 133–145
6. Tennent, G. A., and Pepys, M. B. (1994) *Biochem. Soc. Trans.* **22,** 74–79
7. Emsley, J., White, H. E., O'Hara, B. P., Oliva, G., Srinivasan, N., Tickle, I. J., Blundell, T. L., Pepys, M. B., and Wood, S. P. (1994) *Nature* **367,** 338–345
8. Srinivasan, N., White, H. E., Emsley, J., Wood, S. P., Pepys, M. B., and Blundell, T. L. (1994) *Structure* **2,** 1017–1027
9. Gotschlich, E. C., and Edelman, G. M. (1965) *Proc. Natl. Acad. Sci. U. S. A.* **54,** 558–565
10. Baumann, H., and Gauldie, J. (1994) *Immunol. Today* **15,** 74–80
11. Steel, D. M., and Whitehead, A. S. (1994) *Immunol. Today* **15,** 81–88
12. Schwalbe, R. A., Dahlback, B., Coe, J. E., and Nelsestuen, G. L. (1992) *Biochemistry* **31,** 4907–4915
13. Hicks, P. S., Saunero Nava, L., Du Clos, T. W., and Mold, C. (1992) *J. Immunol.* **149,** 3689–3694
14. Pepys, M. B., and Butler, P. J. (1987) *Biochem. Biophys. Res. Commun.* **148,** 308–313
15. Butler, P. J., Tennent, G. A., and Pepys, M. B. (1990) *J. Exp. Med.* **172,** 13–18
16. Loveless, R. W., Floyd, O. S., Raynes, J. G., Yuen, C. T., and Feizi, T. (1992) *EMBO J.* **11,** 813–819
17. Hind, C. R., Collins, P. M., Renn, D., Cook, R. B., Caspi, D., Baltz, M. L., and Pepys, M. B. (1984) *J. Exp. Med.* **159,** 1058–1069
18. Volanakis, J. E. (1982) *Ann. N. Y. Acad. Sci.* **389,** 235–250
19. Ying, S. C., Gewurz, A. T., Jiang, H., and Gewurz, H. (1993) *J. Immunol.* **150,** 169–176
20. Jiang, H., Siegel, J. N., and Gewurz, H. (1991) *J. Immunol.* **146,** 2324–2330
21. Jiang, H., Robey, F. A., and Gewurz, H. (1992) *J. Exp. Med.* **175,** 1373–1379
22. Bristow, C. L., and Boackle, R. J. (1986) *Mol. Immunol.* **23,** 1045–1052
23. Pepys, M. B., Dyck, R. F., de Beer, F. C., Skinner, M., and Cohen, A. S. (1979) *Clin. Exp. Immunol.* **38,** 284–293
24. de Beer, F. C., Baltz, M. L., Holford, S., Feinstein, A., and Pepys, M. B. (1981) *J. Exp. Med.* **154,** 1134–1139
25. Garcia de Frutos, P., Hardig, Y., and Dahlback, B. (1995) *J. Biol. Chem.* **270,** 26950–26955
26. Hamazaki, H. (1987) *J. Biol. Chem.* **262,** 1456–1460
27. Breviario, F., d'Aniello, E. M., Golay, J., Peri, G., Bottazzi, B., Bairoch, A., Saccone, S., Marzella, R., Predazzi, V., Rocchi, M., Della Valle, G., Dejana, E., Mantovani, A., and Introna, M. (1992) *J. Biol. Chem.* **267,** 22190–22197
28. Lee, G. W., Lee, T. H., and Vilcek, J. (1993) *J. Immunol.* **150,** 1804–1812
29. Vidal Alles, V., Bottazzi, B., Peri, G., Golay, J., Introna, M., and Mantovani, A. (1994) *Blood* **84,** 3483–3493
30. Lee, G. W., Goodman, A. R., Lee, T. H., and Vilcek, J. (1994) *J. Immunol.* **153,** 3700–3707
31. Introna, M., Vidal Alles, V., Castellano, M., Picardi, G., De Gioia, L., Bottazzi, B., Peri, G., Breviario, F., Salmona, M., De Gregorio, L., Dragani, T. A., Srinivasan, N., Blundell, T. L., Hamilton, T. A., and Mantovani, A. (1996) *Blood* **87,** 1862–1872
32. Reid, M. S., and Blobel, C. P. (1994) *J. Biol. Chem.* **269,** 32615–32620
33. Noland, T. D., Friday, B. B., Maulit, M. T., and Gerton, G. L. (1994) *J. Biol. Chem.* **269,** 32607–32614
34. Seery, L. T., Schoenberg, D. R., Barbaux, S., Sharp, P. M., and Whitehead, A. S. (1993) *Proc. R. Soc. Lond. Ser. B Biol. Sci.* **253,** 263–270
35. Schlimgen, A. K., Helms, J. A., Vogel, H., and Perin, M. S. (1995) *Neuron* **14,** 519–526
36. Hsu, Y. C., and Perin, M. S. (1995) *Genomics* **28,** 220–227
37. Tsui, C. C., Copeland, N. G., Gilbert, D. J., Jenkins, N. A., Barnes, C., and Worley, P. F. (1996) *J. Neurosci.* **15,** 2463–2478
38. Laemmli, U. K. (1970) *Nature* **227,** 680–685
39. Wray, W., Boulikas, T., Wray, V. P., and Hancock, R. (1981) *Anal. Biochem.* **118,** 197–203
40. Taketa, K. (1987) *Electrophoresis* **8,** 409–414
41. Pepys, M. B., Dash, A. C., Markham, R. E., Thomas, H. C., Williams, B. D., and Petrie, A. (1978) *Clin. Exp. Immunol.* **32,** 119–124
42. Fiedel, B. A., Simpson, R. M., and Gewurz, H. (1982) *Immunology* **45,** 439–447
43. Tenner, A. J., Lesavre, P. H., and Cooper, N. R. (1981) *J. Immunol.* **127,** 648–653
44. Benfenati, F., and Guardabasso, V. (1984) in *Principles and Methods in Receptor Binding* (Cattabeni, F., and Nicosia, S., eds) pp. 41–63, Plenum Press, New York
45. Johnsson, B., Lofas, S., and Lindquist, G. (1991) *Anal. Biochem.* **198,** 268–277
46. Pepys, M. B., de Beer, F. C., Milstein, C. P., March, J. F., Feinstein, A., Butress, N., Clamp, J. R., Taylor, J., Bruton, C., and Fletcher, T. C. (1982) *Biochim. Biophys. Acta* **704,** 123–133
47. Robey, F. A., Tanaka, T., and Liu, T. Y. (1983) *J. Biol. Chem.* **258,** 3889–3894
48. Robey, F. A., and Liu, T. Y. (1983) *J. Biol. Chem.* **258,** 3895–3900
49. Lin, L., and Liu, T. Y. (1993) *J. Biol. Chem.* **268,** 6809–6815
50. Tennent, G. A., Butler, P. J., Hutton, T., Woolfitt, A. R., Harvey, D. J., Rademacher, T. W., and Pepys, M. B. (1993) *Eur. J. Biochem.* **214,** 91–97
51. Robey, F. A., and Liu, T. Y. (1981) *J. Biol. Chem.* **256,** 969–975
52. Rassouli, M., Sambasivam, H., Azadi, P., Dell, A., Morris, H. R., Nagpurkar, A., Mookerjea, S., and Murray, R. K. (1992) *J. Biol. Chem.* **267,** 2947–2954
53. Nagpurkar, A., and Mookerjea, S. (1981) *J. Biol. Chem.* **256,** 7440–7446
54. Nguyen, N. Y., Suzuki, A., Cheng, S. M., Zon, G., and Liu, T. Y. (1986) *J. Biol. Chem.* **261,** 10450–10455
55. Nguyen, N. Y., Suzuki, A., Boykins, R. A., and Liu, T. Y. (1986) *J. Biol. Chem.* **261,** 10456–10465
56. Turner, M. W. (1996) *Immunol. Today* **17,** 532–538
57. Zahedi, K. (1996) *J. Biol. Chem.* **271,** 14897–14902

[5] L. De Gioia, A. Bastone, and M. Introna, unpublished observations.

Multimer Formation and Ligand Recognition by the Long Pentraxin PTX3: SIMILARITIES AND DIFFERENCES WITH THE SHORT PENTRAXINS C-REACTIVE PROTEIN AND SERUM AMYLOID P COMPONENT

Barbara Bottazzi, Valérie Vouret-Craviari, Antonio Bastone, Luca De Gioia, Cristian Matteucci, Giuseppe Peri, Fabio Spreafico, Mario Pausa, Cinzia D'Ettorre, Elisabetta Gianazza, Aldo Tagliabue, Mario Salmona, Francesco Tedesco, Martino Introna and Alberto Mantovani

J. Biol. Chem. 1997, 272:32817-32823.
doi: 10.1074/jbc.272.52.32817